A First-Principles Quantum Chemical Study of Coenzyme F430: Interplay of Skeletal Stereoisomerism and Conformation in the Stabilization of Nickel(I)

ARTICLE *in* JOURNAL OF THE AMERICAN CHEMICAL SOCIETY · JUNE 2000

Impact Factor: 12.11 · DOI: 10.1021/ja000648b

2 AUTHORS, INCLUDING:

Abhik Ghosh
UiT - The Arctic University of Norway
187 PUBLICATIONS **5,406** CITATIONS

A First-Principles Quantum Chemical Study of Coenzyme F_{430}: Interplay of Skeletal Stereoisomerism and Conformation in the Stabilization of Nickel(I)

Tebikie Wondimagegn[†] and Abhik Ghosh*[,†,‡]

Contribution from the Institute of Chemistry, University of Tromsø, N-9037 Tromsø, Norway, and San Diego Supercomputer Center, University of California - San Diego, La Jolla, California 92093

Received February 22, 2000

Abstract: Nonlocal density functional theory calculations, with full geometry optimization, are reported for the Ni(I) and low-spin Ni(II) forms of high-fidelity models of coenzyme F_{430}, the nickel tetracorphinoid cofactor of methylcoenzyme M reductase (MCR), and its 12,13-diepimer. The diepimer appears to exhibit the conformational characteristics of a typical hydroporphyrin in terms of a strong tendency to adopt highly ruffled conformations and short Ni(II)−N bond distances. In contrast, for native F_{430}, the steric effects of peripheral substituents impose a potent planarizing influence on the ring system. The relative inability to ruffle implies that the N_4 core of F_{430} cannot contract sufficiently to optimally coordinate a small low-spin Ni(II) ion. This appears to be the key factor that results in the stabilization of the larger Ni(I) and high-spin Ni(II) ions by the F_{430} ligand environment. The optimized Ni−N bond distances for the Ni(I)−F_{430} model compound are 198, 200, 203, and 214 pm and span an extremely wide range of 16 pm, which qualitatively reproduces the central feature of the experimental EXAFS results. Understandably, these bond distances are similar to those found in a crystallographic study of a six-coordinate Ni(II) form of MCR. The relatively long Ni−N distances in the optimized geometry of the low-spin Ni(II) form of the F_{430} model compound provide a natural explanation for the enhanced axial ligand affinity of F_{430} and its greater tendency to switch to the high-spin Ni(II) form, relative to its diepimer. Consistent with experiment, the calculations also predict that Ni(II)−diepi-F_{430} is thermodynamically more stable than native Ni(II)−F_{430}. However, for the Ni(I) oxidation level, the two epimers are predicted to be equienergetic. In qualitative agreement with electrochemical measurements, the adiabatic ionization potential of Ni(I)−F_{430} is about 0.2 eV higher than that of Ni(I)−diepi-F_{430}, again reflecting a unique destabilization of low-spin Ni(II) by the F_{430} ligand. Finally, the nickel center in Ni(I)−F_{430} is truly Ni(I): it carries approximately 82% of the molecular unpaired spin, compared to a nickel spin population of only 56% for Ni(I)−diepi-F_{430}.

Introduction

Factor 430 (F_{430},[1] Figure 1) is the nickel tetrahydrocorphinoid[2] cofactor of methylcoenzyme M reductase (MCR), the enzyme that catalyzes the terminal step in the generation of methane by the methanogens, a class of strictly anaerobic archaebacteria. The elucidation of the biochemical pathway of methanogenesis, largely by the research groups of Wolfe[3] and Thauer,[4] over the last quarter-century stands as a landmark in the field of biochemistry. A major goal of current research in this area is to understand the chemistry of F_{430}, to characterize its reactive intermediates, and to describe their electronic structures. A variety of nickel oxidation states, namely, Ni(I), Ni(III),[5] and low- and high-spin Ni(II), have been characterized for F_{430}, and some of them have been proposed as reactive intermediates in the F_{430} reaction cycle.[1] The elucidation of the electronic structures of these intermediates poses many interesting problems for spectroscopists and quantum chemists. A recent EPR and ENDOR study, for example, focused on the electronic structure of the ox1 and ox2 intermediates of F_{430}.[6] This work focuses on the active red1 state,[7] which has been assigned as a tetracoordinate[8] Ni(I) state. In a recent review,[1] Telser has written that "it is clear that Nature has designed F_{430}, using the normal tetrapyrrole building blocks, so as to produce a ligand that optimally generates Ni(I)" and has bemoaned the lack of a "comprehensive theoretical explanation (involving metal orbitals, core size, ligand saturation, ligand distortion, etc.)" of the stabilization of Ni(I). Here we have attempted to achieve such

[†] University of Tromsø. Address correspondence to A.G. at the University of Tromsø. Email: abhik@chem.uit.no.

[‡] San Diego Supercomputer Center.

(1) Telser, J. *Struct. Bonding* **1998**, *91*, 31.

(2) The term corphin describes a hybrid of a porphyrin-type C−N skeleton and corrin-type conjugation: Won, H.; Olson, K. D.; Summers, M. F.; Wolfe, R. S. *Comments Inorg. Chem.* **1993**, *15*, 1.

(3) (a) DiMarco, A. A.; Bobik, T. A.; Wolfe, R. S. *Annu. Rev. Biochem.* **1990**, *59*, 355. (b) Hartzell, P. L.; Wolfe, R. S. *Syst. Appl. Microbiol.* **1986**, *7*, 376. (c) Wolfe, R. S. *Annu. Rev. Microbiol.* **1991**, *45*, 1.

(4) Thauer, R. K. *Microbiology* **1998**, *144*, 2377.

(5) Jaun, B. *Helv. Chim. Acta* **1990**, *73*, 2209.

(6) Telser, J.; Horng, Y.-C.; Becker, D. F.; Hoffman, B. M.; Ragsdale, S. W. *J. Am. Chem. Soc.* **2000**, *122*, 182.

(7) (a) Rospert, S. R.; Böcher, R.; Albracht, S. P. J.; Thauer, R. K. *FEBS Lett.* **1991**, *291*, 371. (b) Rospert, S. R.; Voges, M.; Berkessel, A.; Albracht, S. P. J.; Thauer, R. K. *Eur. J. Biochem.* **1992**, *210*, 101. (c) Albracht, S. P. J.; Ankel-Fuchs, D.; Böcher, R.; Ellermann, J.; Moll, J.; van der Zwaan, J. W.; Thauer, R. K. *Biochim. Biophys. Acta* **1986**, *955*, 86. (d) Krzycki, J. A.; Prince, R. C. *Biochim. Biophys. Acta* **1990**, *1015*, 53. (e) Jaun, B.; Pfaltz, A. *J. Chem. Soc., Chem. Comm.* **1986**, 1327.

(8) For advanced EPR evidence of the tetracoordinate nature of the Ni(I)−F_{430}, see: (a) Holliger, C.; Pierik, A. J.; Reijerse, E. J.; Hagen, W. R. *J. Am. Chem. Soc.* **1993**, *115*, 5651. (b) Telser, J.; Fann, Y.-C.; Renner, M. W.; Fajer, J.; Wang, S.; Zhang, H.; Scott, R. A.; Hoffman, B. M. *J. Am. Chem. Soc.* **1997**, *119*, 733.

10.1021/ja000648b CCC: $19.00
Published on Web 06/24/2000

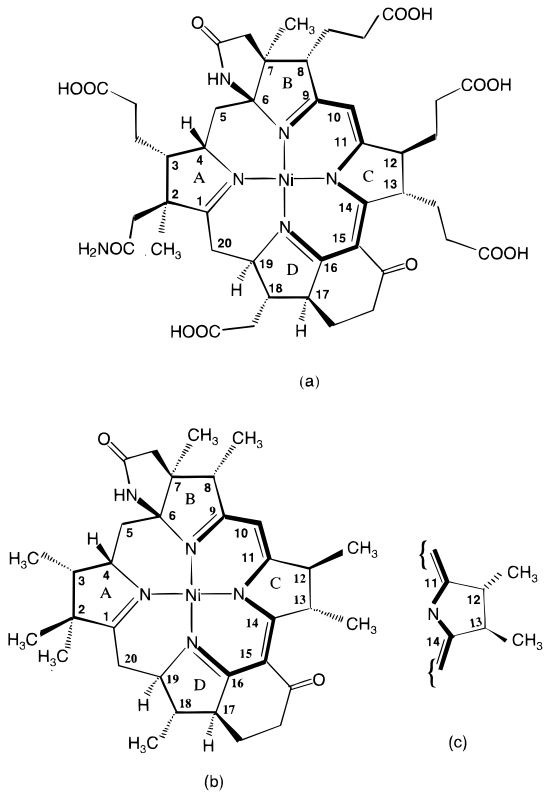

Figure 1. Structure of (a) Ni−F_{430}, (b) Ni−F'_{430}, and (c) Ni−12,13-diepi-F'_{430}.

a theoretical explanation through full geometry optimizations at the level of nonlocal density functional theory (DFT) of the Ni(I) and low-spin Ni(II) forms of carefully chosen models of F_{430} and its 12,13-diepimer (Figure 1). To our knowledge, this is the first major first-principles quantum chemical study of F_{430}.

Until recently, molecular mechanics (MM) methods have been used for most theoretical studies of nonplanar porphyrins and related macrocycles.[9] Presumably, the extreme softness of the potential energy surfaces associated with nonplanar distortions of porphyrin-type macrocycles discouraged the more computationally demanding ab initio and DFT calculations.[10] For F_{430}, a quantum chemical approach is clearly much more desirable than one based on MM because the key goal is to understand the *interplay* of the electronic structure of the nickel center and the conformational characteristics of the tetrahydrocorphinoid ligand. Very recently, DFT has furnished a good understanding of a variety of issues involving nonplanar porphyrins and related macrocycles.[11] Indeed, the present work on F_{430} may be regarded as a culmination of our previous theoretical work on more symmetric, nonplanar porphyrins and hydroporphyrins.[11] Some highlights of this earlier work are as follows.

DFT calculations have provided a fairly comprehensive analysis of the factors responsible for ruffling distortions of porphyrins such as the size of the coordinated ion, axial ligand effects, specific metal(d)−porphyrin(π) orbital interactions, etc.[11a] DFT calculations have also reproduced the experimentally observed, increased propensity of hydroporphyrins to undergo ruffling distortions relative to the porphyrins.[11d,12] Of considerable relevance to this study has been our finding[11d] that seemingly innocent peripheral substituents can dramatically affect and enhance ruffling deformations: for instance, DFT calculations[11] on the Ni(II) complexes of *meso*-tetramethylisobacteriochlorin[13] and *meso*-tetraphenylchlorophin[14] quantitatively reproduce the Ni−N bond distances of ∼190 pm that are observed experimentally and the extremely ruffled macrocycle conformations. If the *meso* substituents are not included in the calculations, the Ni−N bond distances expand significantly to around 194−195 pm, with some reduction of the ruffling.[11d] These and other findings on model tetrapyrroles established the generally excellent performance of DFT in describing the structures and conformations of nonplanar metalloporphyrins. Equally important, they alerted us about the importance of carefully chosen models of F_{430}. For example, unsubstituted Ni(II) tetrahydrocorphin would probably be an inadequate model for F_{430}; instead, we must take into account the alkyl substituents and the exocyclic rings attached to the tetrapyrrole skeleton of F_{430}. As shown in Figure 1, we have done so in our choice of model compounds, F'_{430}, the model of F_{430}, and diepi-F'_{430}, the model of the 12,13-diepimer of F_{430}. We have designed these model compounds by simplifying the acetate, acetamide, and propionate side-chains of F_{430} to methyl groups. This is admittedly a somewhat arbitrary aspect of our theoretical modeling, justified in the end, we believe, by the overall excellent agreement of calculated results with experiment.

The results presented here include the optimized structures of the Ni(I) and low-spin Ni(II) states of F'_{430} and diepi-F'_{430}, the relative energetics of these four species, and the unpaired electron distributions of the two Ni(I) species. The results vividly illustrate the unique conformational characteristics of F_{430}, while indicating that the 12,13-diepimer behaves more like a common hydroporphyrin.

Methods

The calculations used the ADF[15] program system, the PW91 functional, Slater-type triple-ζ plus polarization basis sets, a fine mesh for numerical evaluation of electron repulsion integrals (accint 6.0, with reference to the ADF program manual), and, most importantly for these flexible molecules, tight convergence criteria[16] for atomic forces and displacements in the geometry optimizations (0.0001 hartree for molecular energy, 0.001 hartree/Å for the highest component of the nuclear gradient, and 0.05° for interatomic angles), and a Cray Origin 2000 computer. Not surprisingly, given the size and complete lack of symmetry of the molecules studied, the calculations, although smoothly convergent, were very time-consuming. Researchers intending to repeat these calculations may find it useful, as we did (using PM3 calculations),

(9) (a) Shelnutt, J. A.; Song, X.-Z.; Ma, J.-G.; Jia, S.-L.; Jentzen, W.; Medforth, C. J. *Chem. Soc. Rev.* **1998**, *27*, 31. (b) Zimmer, M. *J. Biomol. Struct. Dyn.* **1993**, *11*, 203. (c) Zimmer, M.; Crabtree, R. H. *J. Am. Chem. Soc.* **1990**, *112*, 1062.

(10) For recent reviews of DFT studies of the molecular structures of porphyrins and metalloporphyrins, see: (a) Ghosh, A. In *The Porphyrin Handbook*; Kadish, K. M., Smith, K. M., Guilard, R., Eds.; Academic: New York, 2000; Vol 7, Chapter 47, pp 1−38. (b) Ghosh, A. *Acc. Chem. Res.* **1998**, *31*, 189.

(11) (a) Vangberg, T.; Ghosh, A. *J. Am. Chem. Soc.* **1999**, *121*, 12154. (b) Ghosh, A.; Gonzalez, E.; Vangberg, T. *J. Phys. Chem. B* **1999**, *103*, 1363. (c) *meso*-Tetrakis(perfluoroalkyl)porphyrins: Wondimagegn, T.; Ghosh, A. *J. Phys. Chem. B*, submitted. (d) Nickel and zinc complexes of hydroporphyrins and chlorophin: Wondimagegn, T.; Ghosh, A. *J. Phys. Chem. B* (Thomas G. Spiro Festschrift), in press.

(12) Barkigia, K. M.; Fajer, J. In *The Photosynthetic Reaction Center*; Deisenhofer, J., Norris, J. R., Eds.; Academic Press: San Diego, 1993; Vol. 2, p 513.

(13) Suh, M. P.; Swepston, P. N.; Ibers, J. A. *J. Am. Chem. Soc.* **1984**, *106*, 5164.

(14) Brückner, C.; Sternberg, E. D.; MacAlpine, J. K.; Rettig, S. J.; Dolphin, D. *J. Am. Chem. Soc.* **1999**, *121*, 2609.

(15) The ADF program is obtainable from: Scientific Computing and Modelling, Department of Theoretical Chemistry, Vrije Universiteit, 1081 HV Amsterdam, The Netherlands.

(16) Convergence criteria for the geometry optimizations were 0.0001 hartrees for the molecular energy, 0.001 for gradients, 0.005 Å for bond distances, and 0.2° for angles.

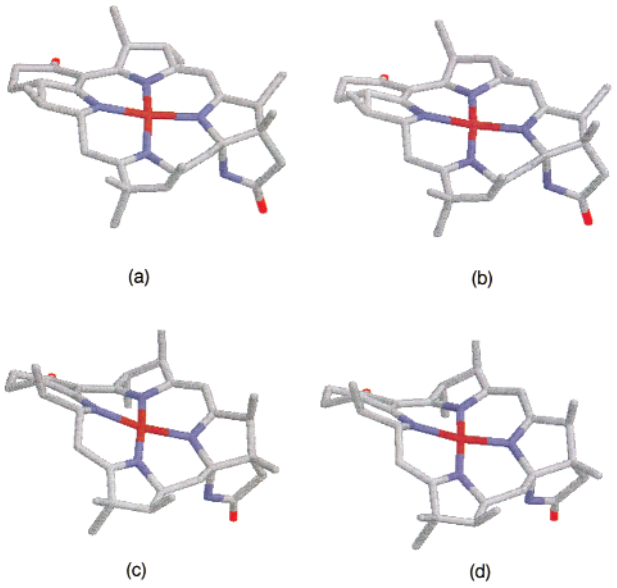

Figure 2. Stick diagrams: (a) Ni(I)−F_{430}, (b) Ni(II)−F'_{430}, (c) Ni(I)−diepi-F'_{430} and (d) Ni(II)−diepi-F'_{430}. Hydrogen atoms are omitted for clarity.

to start the DFT optimizations from semiempirically preoptimized structures. The different results are as follows.

Optimized Geometries and Comparison With X-ray Crystallographic Results

Figure 2 presents stick diagrams of the optimized structures. Figure 3 presents selected distances and angles and Table 1 certain torsion angles from the optimized structures. A measure of ruffling distortions of the tetrapyrrole skeleton is given by the $C_\alpha-N-N-C_\alpha$ torsion angles, involving opposite pyrrole rings, shown in Table 1. As shown qualitatively in Figure 2 and quantitatively in Table 1, the diepi-F'_{430} species are much more ruffled than the F'_{430} species.

The highly ruffled, optimized geometry of Ni(II)−diepi-F'_{430} agrees well the crystallographically determined structure of the 12,13-diepimer of Ni(II) F_{430} pentamethyl ester.[17] (Because the F_{430}-type ligands in question have symmetry-unrelated faces,[18] ruffling inversion[19] would result in diastereomeric conformations. We have checked that the optimized structure of Ni(II)−diepi-F'_{430} corresponds closely to the conformation observed crystallographically.) The Ni−N bond distances (190, 192, 192, and 198 pm) in the optimized structure of Ni(II)−diepi-F'_{430} are fairly typical of low-spin Ni(II) hydroporphyrins. In contrast, the Ni−N distances for Ni(II)−F'_{430} are significantly longer (194, 199, 199, and 205 pm). The diepi-F'_{430} ligand appears to behave as a fairly typical hydroporphyrin in terms of its strong tendency to adopt a highly nonplanar conformation. In contrast, the relative flatness of the F'_{430} complexes is unusual, perhaps unique, for low-spin Ni(II) hydroporphyrins.[11]

For Ni(I)−diepi-F'_{430}, the Ni−N bond distances (195, 196, 199, and 199 pm) are surprisingly close to those of the Ni(II) derivative, Ni(II)−diepi-F'_{430}, suggesting that the diepi-F'_{430} ligand cannot readily "unruffle"/flatten and undergo a core expansion to accommodate the Ni(I) ion. In contrast, the Ni−N bond lengths in Ni(I)−F'_{430} (198, 200, 203, and 214 pm)—values typical of metal−ligand bond lengths in Zn(II) hydroporphyrins[11]—are much longer than those in Ni(I)−diepi-F'_{430}. These bond distances mesh nicely with the known inverse correlation between the N_4 core size and the degree of ruffling deformations.[11] Unlike typical hydroporphyrins, the F'_{430} ligand—and, by extension, F_{430} itself—has an inherently low tendency to ruffle. Accordingly, the N_4 core of F_{430} cannot contract sufficiently to optimally coordinate a small low-spin Ni(II) ion. This appears to be the key factor that results in the stabilization of the larger Ni(I) and high-spin Ni(II) ions by the F_{430} ligand environment. In contrast, an MM study of F_{430} emphasized the flexibility of the macrocycle and found no evidence for an expanded central N_4 core.[20]

Table 1. Selected Dihedral and Torsion Angles (deg)[a]

ruffling angle	Ni(II)−F'_{430}	Ni(I)−F'_{430}	Ni(II)−diepi-F'_{430}	Ni(I)−diepi-F'_{430}
1-N(A)-N(C)−14	13.78	16.35	32.38	28.11
4-N(A)-N(C)−11	20.75	11.94	45.17	41.66
6-N(B)-N(D)−19	36.24	38.83	59.91	42.85
9-N(B)-N(D)−16	27.31	15.91	50.04	57.68
other torsion angles				
N(B)−6−5−4	69.05	71.97	63.90	61.79
N(A)−4−5−6	68.34	64.08	66.82	69.55
N(A)−1−20−19	36.32	44.08	16.78	20.38
N(D)−19−20−1	63.72	66.67	50.89	52.52
N(B)−9−10−11	8.62	9.05	4.33	4.09
N(C)−11−10−9	13.08	10.80	20.70	16.62
N(C)−14−15−16	15.39	15.01	7.24	4.85
N(D)−16−15−14	21.93	21.54	26.29	20.21

[a] A, B, C, and D denote different pyrrole rings (Figure 1). Unless otherwise indicated, the numbers in the left column refer to the carbon atoms in Figure 1.

Recently, Ermler and co-workers have reported a crystallographic strudy of a six-coordinate high-spin Ni(II) state of MCR at 1.45 Å resolution.[21] Although we have not studied the high-spin Ni(II) states in this work, it is reasonable to expect that the optimized Ni(I)−N distances should be similar, to a first approximation, to those found experimentally for the high-spin Ni(II) form of MCR, $MCR_{ox1-silent}$ (whose axial ligands are the side chain oxygen of $Gln^{\alpha 147}$ and the thiol group of coenzyme M) because both Ni(I) and high-spin Ni(II) feature half occupancy of the critical $d_{x^2-y^2}$ orbital. This expectation is indeed fulfilled, and the Ni−N distances observed in the crystal structure are in the range of 199−214 pm, with the longest distance involving the A ring, as in all our optimized geometries. (The nitrogen in the A ring is a neutral imine, while the other central nitrogens have partial anionic character.) The F_{430} tetrapyrrole ring system was also found to be relatively flat, as we find in this study for Ni(I) and low-spin Ni(II)−F'_{430} (compared to 12,13-diepi-F'_{430}). Overall, the available crystallographic results on F_{430} and MCR derivatives further strengthen our faith, based on a number of previous studies, in the quality of structural information derived from DFT calculations.

A key question is what specific factors flatten the F'_{430} ring system and discourage it from ruffling? Given the dramatically different conformational characteristics of F_{430} and its 12,13-dipeimer, we can also rephrase the question as follows: What are the conformational consequences of stereoisomerism at the 12 and 13 positions of the F_{430} tetrapyrrole skeleton? To answer this, we examined the closest interatomic contacts involving the hydrogens of the 12- and 13-methyl substituents of the model

(17) Färber, G.; Keller, W.; Kratky, C.; Jaun, B.; Pfaltz, A.; Spinner, C.; Kobelt, A.; Eschenmoser, A. *Helv. Chim. Acta* **1991**, *74*, 697.

(18) For a recent study on the stereochemical properties of molecular faces, see: Ghosh, A. *Theor. Chem. Acc.* **2000**, in press.

(19) Ozawa, S.; Watanabe, Y.; Morishima, I. *Tetrahedron Lett.* **1994**, *35*, 4141.

(20) Kaplan, W. A.; Suslick, K. S.; Scott, R. A. *J. Am. Chem. Soc.* **1991**, *113*, 9824.

(21) Ermler, U.; Grabarse, W.; Shima, S.; Goubeaud, M.; Thauer, R. K. *Science* **1997**, *278*, 1457.

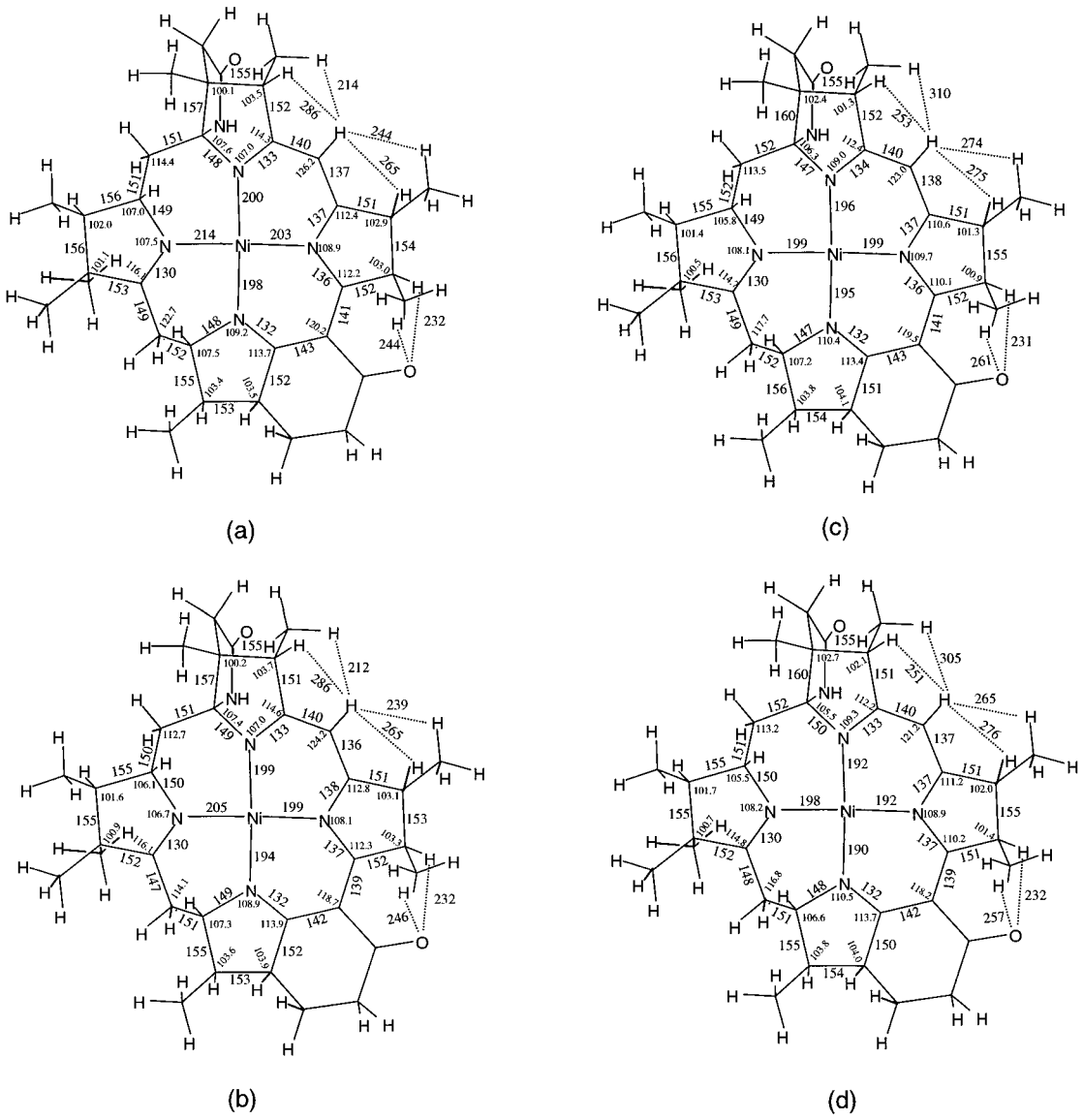

Figure 3. Optimized geometries (pm, deg) of (a) Ni(I)−F′$_{430}$, (b) Ni(II)−F′$_{430}$, (c) Ni(I)−diepi-F′$_{430}$ and (d) Ni(II)−diepi-F′$_{430}$.

complexes studied here. As pointed out by Eschenmoser and co-workers, the propionate group at the 13-position may sterically interact with the carbonyl oxygen of the cyclohexanone ring fused to the tetrapyrrole unit along $C_{15}-C_{16}-C_{17}$ edge.[17] However, among the four molecules optimized for this study, we do not find any major variations in interatomic contacts involving the 13-methyl group or the cyclohexanone oxygen. (This does not necessarily argue against Eschenmoser's proposal: in a future study, we hope to include a longer side-chain at the 13-position to see if it makes a significant difference compared to the results obtained here.) The 12-methyl hydrogens sterically interact with the methine hydrogen at the 10-*meso* position. As far as interatomic contacts are concerned, we find that the largest differences between F′$_{430}$ and diepi-F′$_{430}$ involve the hydrogen at the 10 position. In the case of the F′$_{430}$ complexes, this hydrogen has H···H contacts as short as 212 pm, whereas no such short contacts are found for the diepi-F′$_{430}$ complexes (Figure 3). It appears that the *trans* relative stereochemistry of the 8- and 12-alkyl substituents plays a crucial part in planarizing the F_{430} skeleton. Theoretical studies on the 12- and 13-(mono)epimers of F′$_{430}$ are currently in progress in our laboratory to test this idea.

Discussion of EXAFS Results

The optimized structural data presented here, presumably, bridge a key gap in our knowledge of F_{430}, viz. a detailed structural characterization of Ni(I)−F_{430}. EXAFS has provided some significant and tantalizing clues, but as expected for EXAFS data, they furnish a relatively sketchy picture of the nickel coordination geometry. The DFT structural data on Ni(I)−F′$_{430}$, therefore, may be of considerable interest. Below, we compare the optimized structural data with relevant EXAFS results.

For all of the optimized structures except Ni(I)−F′$_{430}$, the Ni−N distances span a range that is less than 10 pm. The optimized structure of Ni(I)−F′$_{430}$ is exceptional in this regard, with the Ni−N distances spanning a range of 16 pm! Qualitatively, this result reproduces *the* key feature of the EXAFS results, viz. the presence of at least two sets of widely divergent Ni−N distances for Ni(I)−F_{430}.[22] This is an unusual structural feature of Ni(I)−F_{430}, shared by only a handful of model complexes such as Ni(I) octaethylisobacteriochlorin[23] and certain highly saturated Ni(I) tetrazamacrocycles.[24] Because the four

(22) Furenlid, L. R.; Renner, M. W.; Fajer, J. *J. Am. Chem. Soc.* **1990**, *112*, 8987.

Ni−N bonds of F_{430} are symmetry-unrelated, it is important to recognize that EXAFS is not expected to resolve the four different distances. Single-shell EXAFS fits for Ni(II)−F_{430} in water and Ni(II)−12,13-diepi-F_{430} in *N*-methylimidazole, both high-spin $S = 1$ species, yielded average Ni−N distances of 210 and 205 pm, respectively, consistent with our finding that the Ni−N distances in F'_{430} derivatives are longer than those in diepi-F'_{430} derivatives. In contrast, EXAFS data fitting of Ni(I)−F_{430} required the assumption of more than one Ni−N distance and the assumption of two Ni−N bond distances, *in equal proportion*, yielded Ni−N distances of 190 and 204 pm.[21] In a qualitative sense, our calculations are consistent with the EXAFS results, which confirm that the Ni−N bonds in Ni(I)−F_{430} span an unusually broad range. Quantitatively, the agreement between the EXAFS and optimized bond lengths is more modest, the longest Ni−N distance in the optimized geometry of Ni(I)−F'_{430} (214 pm) being 10 pm longer than the longest of the EXAFS bond lengths (204 pm) for Ni(I)−F_{430}. However, in our view, this disagreement between EXAFS and calculated results may not be of particular concern for a number of reasons.

First, we believe that the assumption of two Ni−N bond distances, *in equal proportion*, cannot do justice to the complex variation of Ni−N distances of the type seen in the optimized structure of Ni(I)−F'_{430}.

Second, the relatively long Ni−N bond lengths of about 210 pm, seen in the crystal structure of six-coordinate Ni(II)−MCR and in the EXAFS spectrum of high-spin Ni(II)$(H_2O)_2$−F_{430}, may be regarded as a lower limit for the longest Ni−N distance in Ni(I)−F_{430} [because the higher number of electrons in Ni(I) should make it a larger ion than high-spin Ni(II)]. By this argument, the longest Ni−N distance of 214 pm in the optimized structure of Ni(I)−F'_{430} certainly appears to be qualitatively consistent with experiment.

Third, the EXAFS Ni−N distance of 190[22] pm is too short, in our opinion, for a Ni(I) center. The longer Ni−N distances in the optimized structure of Ni(I)−F'_{430} seem qualitatively more reasonable in light of partial occupancy of the Ni $d_{x^2-y^2}$ orbital.

Finally, these remarks should not be construed as a denigration of the EXAFS studies. There may be shortcomings in our theoretical modeling as well: F'_{430}, after all, is not F_{430}.

Axial Ligand Binding. Compared to Ni(II)−12,13-diepi-F_{430}, Ni(II)−F_{430} exhibits a significantly enhanced propensity to bind axial ligands.[25] Thus, even in water, Ni(II)−F_{430} exists partly as a high-spin bis(aquo) complex whereas Ni(II)−12,13-diepi-F_{430} exists exclusively as a low-spin tetracoordinate species.[25] Ni(II)−12,13-diepi-F_{430} does bind axial ligands, but only those of rather high ligand field strength such as imidazoles and cyanide.[24] The optimized structures shown in Figure 3 readily explain this chemical difference. The relatively long Ni−N bond distances found for Ni(II)−F'_{430} suggest that the Ni(II) ion should have a considerable propensity to switch to the high-spin state, as would happen as a result of axial ligand binding. In contrast, the short Ni−N bonds in diepi-F'_{430} optimized structures suggest that the low-spin Ni(II) state is highly stable and that there is little tendency for the $x^2 - y^2$ orbital to be occupied. It may be recalled that an earlier molecular mechanics study, which did not find an expanded N_4 core for F_{430}, came to the conclusion that the core size was not a significant factor contributing to the enhanced axial ligand affinity of Ni(II)−F_{430}.[20]

Table 2. Gross Atomic Spin Populations from Spin-unrestricted Calculations[a]

Atom	Ni(I)−F'_{430}	Ni(I)−diepi-F'_{430}
Ni	0.8259	0.5624
1	−0.0083	−0.0215
2	0.0041	0.0038
3	0.0036	0.0006
4	0.0028	0.0016
5	0.0007	0.0005
6	0.0036	0.0002
7	0.0022	0.0029
8	0.0052	0.0041
9	−0.0226	0.0487
10	0.0083	−0.0133
11	−0.0214	0.0677
12	0.0053	−0.0017
13	0.0064	−0.0039
14	−0.0155	0.0739
15	0.0085	0.0071
16	−0.0207	−0.0015
17	0.0048	0.0065
18	0.0019	0.0032
19	0.0041	0.0005
20	0.0024	0.0028
N(A)	0.0476	0.0313
N(B)	0.0458	0.0762
N(C)	0.0566	0.0292
N(D)	0.0525	0.0663

[a] Unless otherwise indicated, the numbers in the left column refer to the carbon atoms in Figure 1

Relative Energetics of Different Ni(I) and Ni(II) Species. The energetics of the different species studied in this work nicely complement the structural data described above. As shown by Pfaltz[26] et. al. and Keltjens[27] et. al., Ni(II)−F_{430} is thermally unstable and exists in equilibrium with Ni(II)−diepi-F_{430}, with the latter as the predominant component. Consistent with this observation, we find that Ni(II)−diepi-F'_{430} is more stable than Ni(II)−F'_{430} by 0.21 eV or 4.84 kcal/mol, in agreement with the higher axial ligand affinity of Ni(II)−F_{430} relative to its 12,13-diepimer. In contrast, Ni(I)−diepi-F'_{430} and Ni(I)−F'_{430} are essentially equi-energetic. In other words, the ligand of F'_{430} preferentially stabilizes Ni(I) so as to counterbalance the energy difference between Ni(II)−F'_{430} and Ni(II)−diepi-F'_{430}, in line with the conclusions we reached from the optimized structural data.

The adiabatic ionization potentials of Ni(I)−F'_{430} and Ni(I)−diepi-F'_{430} are 4.52 and 4.32 eV, respectively, where the ionized low-spin Ni(II) cationic states correspond to the optimized geometries of Ni(II)−F'_{430} and Ni(II)−diepi-F'_{430}. In other words, it costs 0.2 eV more to remove an electron from Ni(I)−F'_{430} than from Ni(I)−diepi-F'_{430}, again illustrating the destabilization of low-spin Ni(II) by the ligand of F_{430}. This is qualitatively consistent with electrochemical measurements by Furenlid[28] et. al. and Holliger[8a] et. al., which show that native Ni(II)−F_{430} is more easily reduced (i.e., has a more positive $E_{1/2}$) than its 12,13-diepimer. For example, in *n*-butyronitrile, the reduction potentials of Ni(II)−F_{430} pentamethyl ester and its 12,13-diepimer were found to be −0.71 and −0.79 V, respectively.[28]

(23) (a) Renner, M. W.; Furenlid, L. R.; Stolzenberg, A. M. *J. Am. Chem. Soc*. **1995**, *117*, 293. (b) Renner, M. W.; Furenlid, L. R.; Barkigia, K. M.; Forman, A.; Shim, H. K.; Simpson, D. J.; Smith, K. M.; Fajer, J. *J. Am. Chem. Soc*. **1991**, *113*, 6891.

(24) Furenlid, L. R.; Renner, M. W.; Szalda, D. J.; Fujita, E. *J. Am. Chem. Soc*. **1991**, *113*, 883.

(25) Shiemke, A. K.; Kaplan, W. A.; Hamilton, C. L.; Shelnutt, J. A.; Scott, R. A. *J. Biol. Chem*. **1989**, *264*, 7276.

(26) Pfaltz, A.; Livinston, D. A.; Jaun, B.; Diekert, G.; Thauer, R. K.; Eschenmoser, A. *Helv. Chim. Acta* **1985**, *68*, 1338.

(27) Keltjens, J. T.; Hermans, J. M. H.; Rijsdijk, G. J. F. A.; van der Drift, C.; Vogels, J. D. *Antonie van Leeuwenhoek* **1988**, *54*, 207.

(28) Furenlid, L. R.; Renner, M. W.; Fajer, J. *J. Am. Chem. Soc*. **1990**, *112*, 8987.

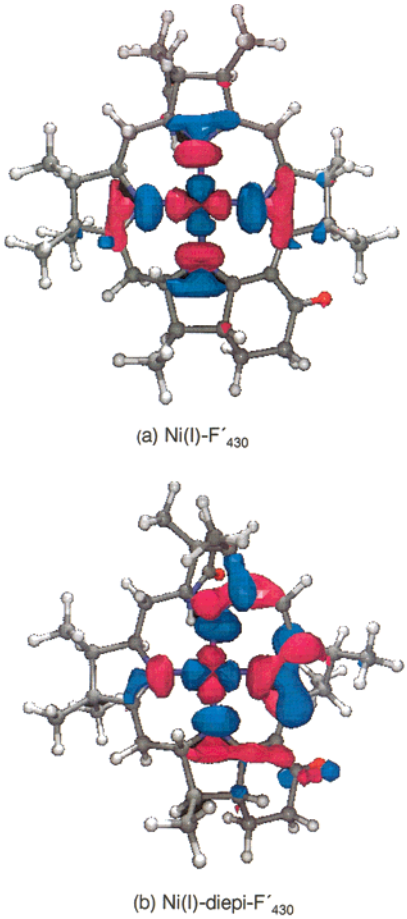

Figure 4. Open-shell molecular orbitals of Ni(I)−F′$_{430}$ and Ni(I)−diepi-F′$_{430}$.

Unpaired Electron Distributions. There are relatively few chemical models of Ni(I)−F_{430}. One-electron reduction of Ni(II) porphyrins and hydroporphyrins typically leads to Ni(II) ligand π-anion radicals. A notable exception is nickel octaethylisobacteriochlorin (NiOEiBC), for which the anionic state, $[NiOEiBC]^-$,[8b,23] corresponds to a Ni(I) state and has been described as an "exceptional nucleophile".[29] Certain other highly saturated tetraazamacrocyclic ligands also stabilize the Ni(I) oxidation state. However, overall, Ni(I) complexes of porphyrin-type ligands are rare. Thus, another critical test of the calculations described here is whether they predict a "true" Ni(I) state for reduced F_{430}.

Table 2 presents the calculated unpaired spin populations for Ni(I)−F′$_{430}$ and Ni(I)−diepi-F′$_{430}$ and Figure 4 the open-shell orbitals of the two compounds. For Ni(I)−F′$_{430}$, the calculated spin density distribution exactly corresponds to that expected for a Ni(I) complex. Approximately 82% of the unpaired spin is localized in the Ni $d_{x^2-y^2}$ orbital, with the remainder distributed almost equally on the four central nitrogens. The spin population on the central nitrogens originates through simple σ-bonding involving the Ni $d_{x^2-y^2}$ orbital and the nitrogen lone pairs.

For Ni(I)−diepi-F′$_{430}$, the spin population on the nickel is significantly less, about 56%. As in the case of Ni(I)−F′$_{430}$, the central nitrogens carry modest unpaired spin populations (2−7%), but certain skeletal carbon atoms also carry significant amounts unpaired spin density (up to 7%). In other words, although "Ni(I)−diepi-F′$_{430}$" has some Ni(I) character, it also has significant ligand anion radical character.

(29) Helvenston M. C.; Castro, C. E. *J. Am. Chem. Soc.* **1992**, *114*, 8490.

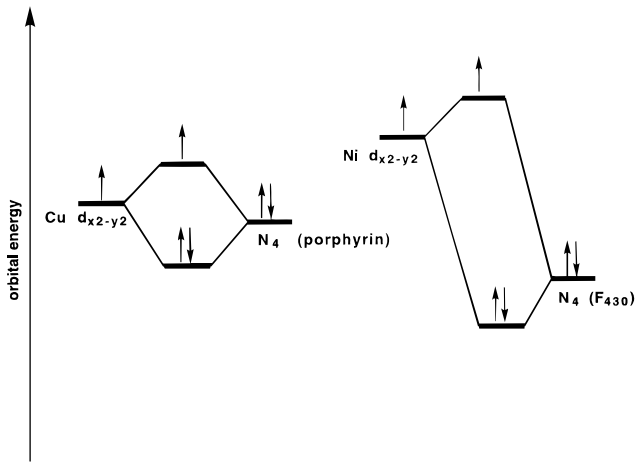

Figure 5. Orbital interaction diagrams for metal($d_{x^2-y^2}$)-macrocycle σ interaction. The orbital denoted as N_4 may be regarded as a symmetry-adapted ligand group orbital formed from the macrocycle in-plane lone pairs.

Because mononuclear Ni(I) and Ni(III) complexes are both $S = {}^1/_2$ species, experimentalists have sought to determine spectroscopic signatures that distinguish the two oxidation states. Differences in EPR spectra have led to the conclusion that Ni(III) complexes typically have a $(z^2)^1$ occupation, whereas Ni(I) complexes are generally $(x^2 - y^2)^1$.[7e,8] However, Bocian[30] and co-workers have shown that Ni(III) porphyrins can exhibit both $(z^2)^1$ and $(x^2 - y^2)^1$ occupancies, depending on the axial ligands. EPR measurements have suggested that the unpaired electrons in $[Ni^{III}(TPP)(Py)_2]^+$ and $[Ni^{III}(TPP)(CN)_2]^-$ (TPP = tetraphenylporphyrin) occupy a metal d_{z^2} orbital and a metal $d_{x^2-y^2}$ orbital, respectively. Our theoretical calculations have also confirmed this assignment. The relevance of these results to the present problem is that both Ni(I)−F_{430} and $[Ni^{III}(TPP)(CN)_2]^-$ have $(x^2 - y^2)^1$ unpaired electron occupancies and, accordingly, it is instructive to compare their spin density profiles.

DFT calculations on $[Ni^{III}(P)(CN)_2]^-$ at the same level of theory as in this study predict a nickel spin population of 0.65 and a porphyrin nitrogen spin population of 0.08 per nitrogen.[31] The nickel spin population is smaller and the porphyrin spin population is larger than those found here for Ni(I)−F′$_{430}$. This difference is understandable because porphyrin, as a dianionic ligand, should harbor more of the radical character the high-valent Ni(III) center. In contrast, the low-valent Ni(I) center is less effective in delocalizing its unpaired electrons in a σ fashion to the F_{430} nitrogens.

It is also instructive to compare the spin density profile of Ni(I)−F′$_{430}$ with that of Cu(II) porphyrins, also d^9 complexes. For Cu(II) porphyrins, the metal center typically carries a spin population of about 50%,[32] significantly less than that for Ni(I)−F′$_{430}$. This can be understood through a qualitative orbital interaction diagram (Figure 5). Figure 5 shows that the $d_{x^2-y^2}$ orbital of Ni(I) is at a higher energy than that of Cu(II) whereas the σ-bonding N_4 "ligand group orbital" of the uninegative F_{430}-like ligand is at a lower energy than the analogous orbital of the dinegative porphyrin ligand. This, as suggested in Figure 5, indicates that the open-shell MO of Ni(I)−F′$_{430}$ should have a significantly higher metal character relative to the open-shell

(30) Seth, J.; Palaniappan, V.; Bocian, D. F. *Inorg. Chem.* **1995**, *34*, 2201.

(31) Ghosh, A.; Wondimagegn, T.; Gonzalez, E.; Halvorsen, I. *J. Inorg. Biochem.* **2000**, *78*, 79.

(32) (a) Brown, T. G.; Hoffman, B. M. *Mol. Phys.* **1980**, *39*, 1073. (b) Ghosh, A.; Wondimagegn, T. Unpublished results.

MO of copper porphyrins. This is consistent with ^{14}N ENDOR-derived spin density profiles for MCR_{red1} and CuTPP (TPP = tetraphenylporphyrin).[6]

On the Question of Ni(III)−F_{430} Intermediates for MCR. At the time this paper is being revised after initial review, we have also obtained some results on Ni(III)−F_{430} model compounds. These are of interest because Ermler and co-workers have proposed a Ni(III)−CH_3 intermediate for the reaction cycle of MCR. How might the F_{430} ligand stabilize both low-valent Ni(I) and high-valent Ni(III) intermediates? One might be tempted to invoke a special flexibility of the F430 ligand, as suggested by an MM study. However, preliminary calculations on a Ni(III)−CH_3 derivative of F'_{430} (with an axial formamido-*O* ligand) suggest otherwise. Like $Ni^{III}(TPP)(CN)_2]^-$, this Ni(III)−CH_3 species has an $(x^2 - y^2)^1$ configuration. Thus, it appears that Nature has specifically tailored the molecular architecture of F_{430} for the occupancy of the nickel $d_{x^2-y^2}$ orbital and hence relatively long Ni−N bonds. This is consistent with the mechanism proposed by Ermler and co-workers for MCR which involves Ni(I), high-spin Ni(II), and Ni(III) intermediates, but excludes the most common spin state of nickel, low-spin Ni(II).

Conclusions

The principal conclusions of this work are as follows.

1. On the basis of model calculations, it appears that the 12,13-diepimer of F_{430} exhibits the conformational characteristics of an ordinary hydroporphyrin in terms of its strong tendency to adopt highly ruffled conformations.

2. In contrast, the steric effects of peripheral substituents, particularly the stereochemistry at the 12 and 13 positions of the native coenzyme, impose a potent planarizing constraint on the F_{430} ring system. The relative inability to ruffle implies that the N_4 core of F_{430} cannot contract sufficiently to optimally coordinate a small low-spin Ni(II) ion. This appears to be the key factor that results in the stabilization of the larger Ni(I) and high-spin Ni(II) ions by the F_{430} ligand environment. This also provides a natural explanation for the enhanced axial ligand affinity of Ni(II)−F_{430}, relative to its 12,13-diepimer.

It is somewhat ironic that F_{430}, a molecule that has inspired countless studies of nonplanar porphyrinoids, may owe its unique chemistry to a relative inability to adopt strongly nonplanar conformations.

3. The optimized geometry of a Ni(I) F_{430} model compound has provided the first detailed picture, albeit quantum chemically derived, of the molecular structure of the active Ni(I) state of the coenzyme. The optimized Ni−N distances of 198, 200, 203, and 214 pm span a surprisingly wide range of 16 pm, which qualitatively reproduces the experimental EXAFS finding of two distinct Ni−N distances for Ni(I)−F_{430}. Understandably, these bond distances are similar to those found in a crystallographic study of a six-coordinate Ni(II) form of MCR, $MCR_{ox1-silent}$.

4. Consistent with experiment, the calculations predict that Ni(II)−diepi-F_{430} is thermodynamically more stable than native Ni(II)−F_{430}. In contrast, for the Ni(I) oxidation level, the two epimers are predicted to be equi-energetic.

5. In qualitative agreement with electrochemical measurements, the adiabatic ionization potential of Ni(I)−F_{430} is about 0.2 eV higher than that of Ni(I)−diepi-F_{430}, again reflecting the unique destabilization of low-spin Ni(II) by the F_{430} ligand.

6. For Ni(I)−F'_{430}, the nickel center is truly Ni(I): it carries approximately 82% of the molecular unpaired spin, compared to a nickel spin population of only 56% for Ni(I)−diepi-F_{430}.

7. For a Ni(III)−CH_3 derivative of F'_{430}, preliminary calculations predict an $(x^2 - y^2)^1$ electronic configuration, an unusual but known configuration for Ni(III), suggesting that the F_{430} ligand has been specifically engineered for occupancy of the Ni $d_{x^2-y^2}$ orbital.

In our view, the calculations have provided a satisfying, self-consistent picture of the electronic and geometric structures and energetics of a number of F_{430} derivatives. Gratifyingly, all relevant experimental results, obtained from protein and small-molecule X-ray crystallography, EXAFS, observations on the thermodynamic stabilities of stereoisomeric F_{430} derivatives, electrochemistry, and EPR, confirm and mesh seamlessly with the theoretically obtained picture, lending credence to our belief that, eventually, the more predictive aspects of this study, especially those describing the Ni(I) state of the coenzyme, will also be experimentally confirmed. We plan to report our results on other F_{430} intermediates in the foreseeable future.

Acknowledgment. This work was supported by the Norwegian Research Council, the VISTA program of Statoil (Norway), and a Senior Fellowship (A.G.) of the San Diego Supercomputer Center. We thank two anonymous reviewers for their detailed comments.

Supporting Information Available: Optimized coordinates of the different molecules are given herein (PDF). This material is available free of charge via the Internet at http://pubs.acs.org.

JA000648B